Plasmonic and bolometric terahertz detection by graphene field-effect transistor

A. V. Muraviev,[1,a)] S. L. Rumyantsev,[1,2] G. Liu,[3] A. A. Balandin,[3] W. Knap,[4] and M. S. Shur[1]
[1]*ECSE and PAPA Department, Rensselaer Polytechnic Institute, Troy, New York 12180, USA*
[2]*Ioffe Physical-Technical Institute, Russian Academy of Sciences, St. Petersburg 194021, Russia*
[3]*Nano-Device Laboratory, Department of Electrical Engineering, Bourns College of Engineering, University of California–Riverside, Riverside, California 92521, USA*
[4]*Laboratoire Charles Coulomb and TERALAB, Université Montpellier 2 and CNRS, 34950 Montpellier, France*

(Received 29 May 2013; accepted 23 September 2013; published online 30 October 2013)

Polarization dependence analysis of back-gated graphene field-effect transistor terahertz responsivity at frequencies ranging from 1.63 to 3.11 THz reveals two independent mechanisms of THz detection by graphene transistor: plasmonic, associated with the transistor nonlinearity, and bolometric, caused by graphene sheet temperature increase due to THz radiation absorption. In the bolometric regime, electron and hole branches demonstrate a very different response to THz radiation, which we link to the asymmetry of the current-voltage characteristics temperature dependence with respect to the Dirac point. Obtained results are important for development of high-efficiency graphene THz detectors. © *2013 AIP Publishing LLC*. [http://dx.doi.org/10.1063/1.4826139]

Graphene field effect transistors[1–7] have emerged as promising candidates for THz applications, including detection, mixing, and generation of THz radiation.[8–15] The discussed mechanisms of interaction between 2D electron gas in graphene sheet and terahertz radiation have been traditionally considered plasmonic, based of non-linear properties of plasma waves excitations in 2D electron gas.[8–14] However, experimental observations are not always in direct agreement with the expected effects due to the contribution of other mechanisms of terahertz detection, which are discussed in this paper. In particular, non-plasmonic mechanism of detection by graphene devices, associated with bolometric heating, has been theoretically proposed in Ref. 15.

The idea of using field-effect transistors (FETs) for detection of THz radiation was proposed in Ref. 16. The mechanism of detection depends on the $\omega_0\tau$ product, where $\omega_0 = \pi s/2L_g$ is the fundamental plasma frequency, s is the plasma wave velocity, L_g is the transistor (gate) length, and τ is the momentum relaxation time. In the regime when $\omega_0\tau \gg 1$, the FET operates as a resonant detector. The regime when $\omega_0\tau \ll 1$ corresponds to a non-resonant detection. The amplitude of the non-resonant response depends on the device design and material, bias parameters, and frequency.[17] For low frequencies and long gate devices, a phenomenological formula relates the expected detector signal with the channel conductivity[18]

$$\Delta u \propto \frac{1}{\sigma}\frac{d\sigma}{dV_g}, \tag{1}$$

where σ is the channel conductance and V_g is the gate voltage. For a more general case, the expression for Δu is given by Ref. 19.

Equation (1) is in a good agreement with experimental observations of non-resonant detection of graphene transistor at 0.3 THz.[11] In this work, we study terahertz detection by a bottom-gate graphene transistor at frequencies of 1.63, 2.55, and 3.11 THz and show that the same device operates in two different detection regimes: plasmonic and bolometric.

Single-layer and multi-layer graphene transistors were fabricated using the standard approach of mechanical exfoliation from bulk highly oriented pyrolytic graphite. The p-type highly doped Si wafers with resistivity about 0.003 Ω cm covered with 300-nm thermally grown SiO_2 served as a substrate and back-gate for exfoliated graphene. Graphene flakes were identified using micro-Raman spectroscopy. The 10-nm Cr/100-nm Au source and drain contacts were deposited on graphene by the electron beam evaporation. Fig. 1(a) shows the configuration of the device with three drain-source contacts, which form two independent transistors with the distances between source and drain contacts $L_{g1} = 1.9\,\mu$m and $L_{g2} = 7.9\,\mu$m. The room temperature mobility of the charge carriers obtained from current-voltage characteristics in both devices varied from 3000 to 10000 cm^2/Vs for both electrons and holes.[20]

The tested graphene device (Fig. 1(a)) was installed on a probe station in the focal plane of a 2 in. 90° off-axis parabolic gold mirror. The mirror focused the radiation of the CW optically pumped THz gas laser SIFIR-50 (Coherent, Inc.) on the device so that the propagation direction of the incident beam was normal to the device plane. The focused spot size was close to the diffraction limit. The laser beam was modulated by a chopper at 200 Hz, and the transistor response was measured as a radiation induced change of the voltage drop across a 10 kΩ load resistor in series with the source-drain channel of the device. A wire grid polarizer controlled polarization of the incident THz radiation. The angle θin Fig. 1(a) is the angle between the electric field of the electromagnetic wave and the orientation of the source electrode.

The device with the shorter channel $L_{g1} = 1.9\,\mu$m was designed to have perpendicular orientations of the source and drain contact leads, which worked as antennas for the

a)Email: amuravie@gmail.com

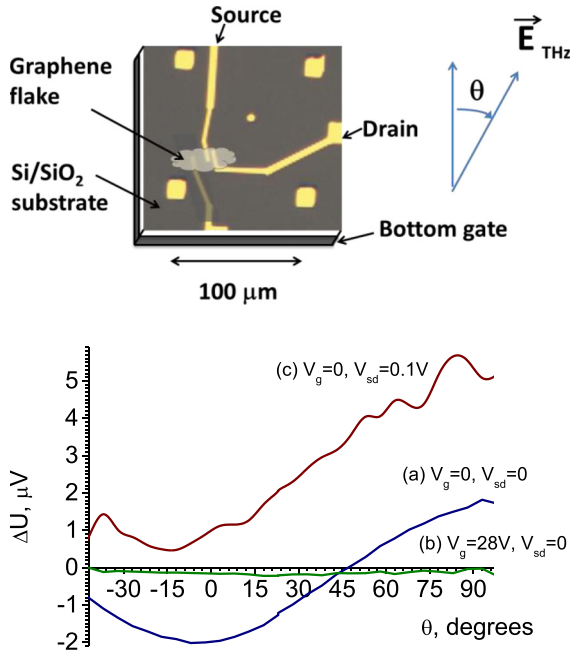

FIG. 1. Top: Diagram of tested graphene device. The width of the graphene channel is W = 3.5-4 μm, the distance between the contacts is $L_{g1} = 1.9\ \mu$m and $L_{g2} = 7.9\ \mu$m. The device with $L_{g1} = 1.9\ \mu$m used in experiments is indicated by brighter contact leads. θ is the polarization angle of incident terahertz radiation. Bottom: Polarization dependence of the graphene device response with $L_{g1} = 1.9\ \mu$m on THz radiation for three bias configurations: (a) $V_g = 0$, $V_{sd} = 0$; (b) $V_g = 28$ V (near Dirac point), $V_{sd} = 0$; (c) $V_g = 0$, $V_{sd} = 100$ mV. Laser line 2.55 THz, emitted laser power 130 mW. Absolute value of the response was recalibrated as for total incident laser power, in order of taking into account the reduction of incident intensity at polarizer rotation.

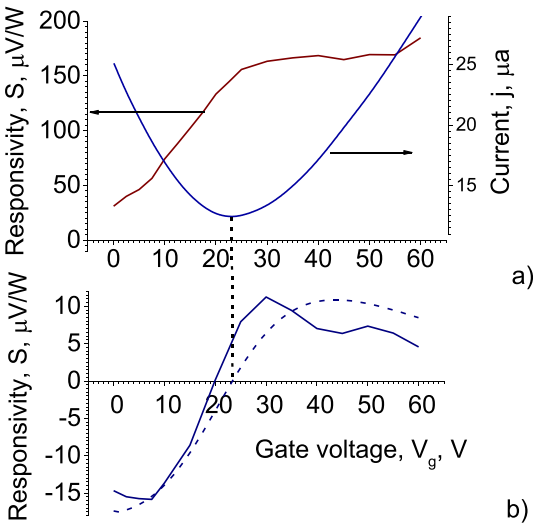

FIG. 2. (a) Responsivity of the device with $L_{g1} = 1.9\ \mu$m on 2.55 THz radiation at $V_{sd} = 100$ mV bias and polarization angle $\theta = 23°$ (left); the absolute value of the responsivity was recalibrated for configuration with constant current (infinite load resistor) in order to compensate distortion of the dependence caused by the change of channel impedance with V_g. Transfer current-voltage characteristics of the device measured at $V_{sd} = 100$ mV (right). (b) Responsivity at $V_{sd} = 0$; dashed line shows theoretical response dependence.

incident THz radiation. The length of these contact leads, shown in Fig. 1(a), was comparable to typical waist of focused THz beam at the frequencies used in the experiment. Based on the lead orientation, we conclude that the THz excitation was primarily induced between the source and gate for polarization angle $\theta \sim 0°$ and between the drain and gate for polarization angle $\theta \sim 90°$. Due to the reflection from a highly doped substrate, THz field strength in the active plane of the devise was suppressed, which, however, should not affect the overall pattern of the THz response, including polarization dependences (We estimate the skin depth of THz penetration inside the substrate as several microns.).

Fig. 1(b) shows measured polarization dependence of the device THz response as a function of the polarization angle θ. The sign of the response in the case of applying bias current through the device corresponds to the decrease of the sample conductivity.

Without drain current (curve "a") the measured responsivity demonstrates well pronounced cosine-like polarization dependence with positive maximum at $\theta = 90°$ and negative absolute value maximum at $\theta = 0°$ (Fig. 1(b)), in accordance with alignment of incident THz radiation polarization along either source or drain gold current lead. The response is changing sign at $\theta \sim 45°$, which corresponds to symmetrical polarization orientation with respect to the source and drain current leads. In contrast to the dipole-like polarization diagram observed in Ref. 11, this dependence has quadrupole pattern. Curve "b" represents the same dependence at $V_g = 28$ V, demonstrating absence of the THz response in Dirac point.

In the presence of the drain current (curve "c") the response acquires an additional component, which does not depend on polarization. This fact suggests the existence of two independent mechanisms of the device response, which we analyze below.

Fig. 2 compares the measured unbiased and biased responses with the device transfer current-voltage characteristics. The measurement has been performed for the laser frequency 2.55 THz and polarization angle $\theta \sim 23°$. The observed unbiased responsivity dependence (Fig. 2(b), solid line) is in good agreement with normalized dependence of the expected response (dashed line), which has been calculated using Eq. (1) by differentiating the experimental current voltage characteristics shown in Fig. 2(a) (see also Ref. 21). As seen, the change of the response sign occurs at the gate voltage close to the charge neutrality (Dirac) point where the derivative $d\sigma/dV_g = 0$. In the presence of the drain current (biased, Fig. 2(a)) both the response symmetry in respect to Dirac point for V_g, as well as the polarization dependence symmetry, are lost.

The same measurements were repeated on the same sample for two other frequencies: 1.63 THz and 3.11 THz (Fig. 3), which generally show similar behavior, except for abnormal dependence of the response observed without current at 3.11 THz. Different sign of the 3.11 THz response dependence in the vicinity of the Dirac point is explained by almost orthogonal polarization of incident radiation used for 3.11 THz laser line in accordance with Fig. 1(b). However, behavior of the dependence at high gate biases in the respect to Dirac point is unusual and is not described in terms of Eq. (1), which is a subject for future study.

The absolute values of the measured responsivity presented in Figs. 2 and 3 used direct reference to laser emitted power without adjustments associated with the factor of coupling efficiency. The observed responsivity levels were

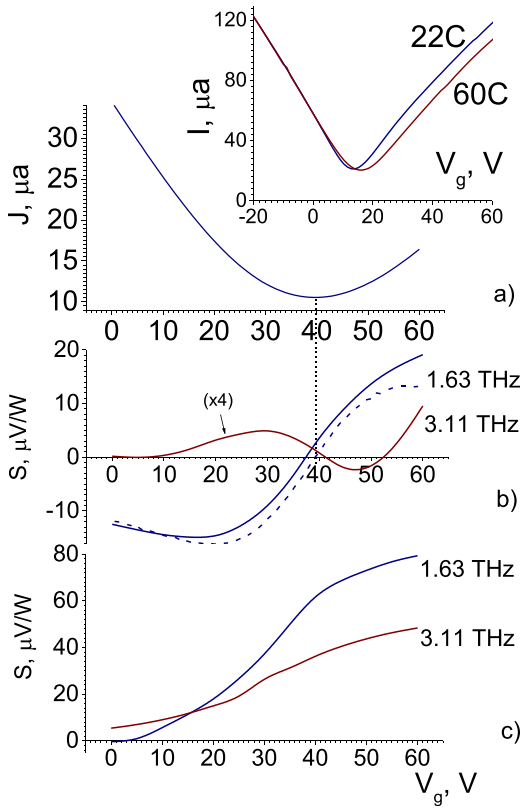

FIG. 3. Transfer current-voltage characteristics (a) of the device with $L_{g1} = 1.9\ \mu$m ($V_{sd} = 100$ mV) and device responsivity at 1.63 THz and 3.11 THz for unbiased (b) and biased (c) cases, analogous to shown in Fig. 2. The absolute value of the responsivity was recalibrated the same way as in Fig. 2. Polarization angle of incident radiation was $\theta = 23°$ for 1.63 THz laser line and $\theta = 95°$ for 3.11 THz laser line. Dashed line shows theoretical response dependence. Note that the device Dirac point here has been shifted towards higher gate voltages in respect to the data in Fig. 2 possibly due to recharging of long-living impurity centers. The inset in Fig. 3(a) shows transfer IV characteristics of similar graphene FET from the same series, measured at different substrate temperatures.

comparable for 1.63 THz and 3.11 THz in the presence of the DC drain-to-source current (Fig. 2(a)), while at zero current the response at 3.11 THz was about an order of magnitude weaker.

This strong frequency dependence of the response in the unbiased case and very well pronounced polarization dependence are evidence of the plasma wave mechanism of the THz detection similar to observed in traditional field effect transistors. Possible thermoelectric effects on graphene-metal interfaces, which may result in similar response pattern due to different heating of the source and drain electrodes by the THz radiation, in our case must be negligible because of high thermal conductivity of graphene sheet. In contrast, the device response appearing in the presence of the DC drain-to-source current is not polarization dependent and has weak frequency dependence, which we associate with bolometric mechanism of detection, caused by absorption of the THz radiation in the conductive substrate and graphene sheet itself, and the resulting change of the sample conductivity due to the temperature induced shift of Dirac point. Since both orthogonal polarizations lead to the same sign of the response for the bolometric mechanism, the dependence on polarization vanishes. The comparison with independently measured temperature dependences of the sample conductivity gives the estimate of graphene sheet temperature change due to THz radiation to be on the order of 50 mK. The measured differential thermal resistivity of this graphene device in the electron branch of transfer IV characteristics has an order of 5 Ω/K, rather close to typical values for GaN heterostructure microbolometers.[22] The observed asymmetry of the bolometric response in respect to Dirac point is explained by the asymmetry of the transfer current-voltage characteristics temperature dependence, which is shown in the inset to Fig. 3(a). This kind of electron-hole asymmetry has been seen before by multiple authors (for example, see Ref. 23) and is associated with long-living impurity centers.

In conclusion, we observed two different patterns of terahertz detection by a graphene bottom-gate field-effect transistor. The first one features pronounced frequency dependence, quadrupole polarization diagram, and anti-symmetry in respect to Dirac point, which we associate with the plasma-wave rectification mechanism, based on nonlinearities of the electron transport in field effect transistors. The second mechanism is polarization independent, weakly dependent on frequency bolometric effect which we associate with the change of graphene sheet temperature due to direct absorption of the incident THz radiation. The bolometric response is not symmetric for electrons and holes due to simultaneous decrease of carrier mobility and a shift of the Dirac point with temperature, which is in agreement with temperature dependence of the device transverse current-voltage characteristics.

The work at RPI was supported by Qatar University under contract NPRP 09-1211-2-475. A.A.B. acknowledges support of the NSF project CCF 1217382: Collaborative Research: Graphene Circuits for Analog, Mixed-Signal, and RF Applications and SRC – DARPA Center for Function Accelerated nanoMaterial Engineering (FAME). S.L.R. acknowledges support from the Russian Fund for Basic Research (RFBR). The authors gratefully acknowledge the support of Partner University Fund (ref. PUF/CP/PB01). We are very thankful to Alexey Gutin for his help with manuscript preparation.

[1]K. S. Novoselov, A. K. Geim, S. V. Morozov, D. Jiang, Y. Zhang, S. V. Dubonos, I. V. Grigorieva, and A. A. Firsov, Science **306**, 666 (2004).
[2]Y. B. Zhang, Y. W. Tan, H. L. Stormer, and P. Kim, Nature **438**, 201 (2005).
[3]S. Stankovich, D. A. Dikin, G. H. B. Dommett, K. M. Kohlhaas, E. J. Zimney, E. A. Stach, R. D. Piner, S. T. Nguyen, and R. S. Ruoff, Nature **442**, 282 (2006).
[4]S. V. Morozov, K. S. Novoselov, M. I. Katsnelson, F. Schedin, D. C. Elias, J. A. Jaszczak, and A. K. Geim, Phys. Rev. Lett. **100**, 016602 (2008).
[5]K. I. Bolotin, K. J. Sikes, J. Hone, H. L. Stormer, and P. Kim, Phys. Rev. Lett. **101**, 096802 (2008).
[6]A. A. Balandin, S. Ghosh, W. Bao, I. Calizo, D. Teweldebrhan, F. Miao, and C. N. Lau, Nano Lett. **8**, 902 (2008).
[7]A. A. Balandin, Nature Mater. **10**, 569 (2011).
[8]V. Ryzhii, T. Otsuji, M. Ryzhii, and M. S. Shur, "Double graphene-layer plasma resonances terahertz detector," J. Phys. D: Appl. Phys. **45**, 302001 (2012).
[9]V. Ryzhii, A. Satou, T. Otsuji, M. Ryzhii, N. Ryabova, S. O. Yurchenko, and M. S. Shur, "Graphene-based electro-optical modulator: Concept and analysis," in *Proceedings of the IEEE International Meeting for Future of Electron Devices, Kansai* (IMFEDK, 2012), p. 2.
[10]T. Otsuji, S. A. B. Tombet, A. Satou, H. Fukidome, M. Suemitsu, E. Sano, V. Popov, M. Ryzhii, and V. Ryzhii, "Graphene-based devices in terahertz science and technology," J. Phys. D: Appl. Phys. **45**, 303001 (2012).

[11]L. Vicarelli, M. S. Vitiello, D. Coquillat, A. Lombardo, A. C. Ferrari, W. Knap, M. Polini, V. Pellegrini, and A. Tredicucci, "Graphene field-effect transistors as room-temperature terahertz detectors," Nature Mater. **11**, 865 (2012).
[12]V. V. Popov, O. V. Polischuk, A. R. Davoyan, V. Ryzhii, T. Otsuji, and M. S. Shur, "Amplification of terahertz radiation by stimulated emission of plasmons in graphene," in IRMWW-THz, 2013.
[13]M. Ryzhii, T. Otsuji, A. Satou, V. Ryzhii, V. Mitin, and M. S. Shur, "Plasmonic effects in terahertz photomixing in double-graphene-layer heterostructures," in PIERS, Stockholm, 2013.
[14]V. Ryzhii, T. Otsuji, M. Ryzhii, V. G. Leiman, S. O. Yurchenko, V. Mitin, and M. S. Shur, "Effect of plasma resonances on dynamic characteristics of double graphene-layer optical modulator," J. Appl. Phys. **112**, 104507 (2012).
[15]V. Ryzhii, T. Otsuji, M. Ryzhii, N. Ryabova, S. O. Yurchenko, V. Mitin, and M. S. Shur, "Graphene terahertz uncooled bolometers," J. Phys. D: Appl. Phys. **46**, 065102 (2013).
[16]M. I. Dyakonov and M. S. Shur, "Plasma wave electronics: Novel terahertz devices using two dimensional electron fluid," IEEE Trans. Electron Devices **43**(10), 1640–1645 (1996).
[17]W. Knap, M. Dyakonov, D. Coquillat, F. Teppe, N. Dyakonova, J. Lusakowski, K. Karpierz, M. Sakowicz, G. Valusis, D. Seliuta, I. Kasalynas, A. El Fatimy, Y. M. Meziani, and T. Otsuji, "Field effect transistors for terahertz detection: physics and first imaging applications," Int. J. Infrared Millim. Terahz. Waves **30**, 1319 (2009).
[18]M. Sakowicz, M. B. Lifshits, O. A. Klimenko, F. Schuster, D. Coquillat, F. Teppe, and W. Knap, "Terahertz responsivity of field effect transistors versus their static channel conductivity and loading effects," J. Appl. Phys. **110**, 054512 (2011).
[19]V. Yu. Kachorovskii, S. L. Roumyantsev, W. Knap, and M. Shur, "Performance limits for field effect transistors as terahertz detectors," Appl. Phys. Lett. **102**, 223505 (2013).
[20]S. Rumyantsev, G. Liu, W. Stillman, M. Shur, and A. A. Balandin, "Electrical and noise characteristics of graphene field-effect transistors: Ambient effects, noise sources, and physical mechanisms," J. Phys.: Condens. Matter **22**, 395302 (2010).
[21]T. A. Elkhatib, V. Yu. Kachorovskii, W. J. Stillman, S. Rumyantsev, X.-C. Zhang, and M. S. Shur, "Terahertz response of field-effect transistors in saturation regime," Appl. Phys. Lett. **98**, 243505 (2011).
[22]J. K. Choi, V. Mitin, R. Ramaswamy, V. Pogrebnyak, M. Pakmehr, A. Muravjov, M. Shur, J. Gill, I. Medhi, B. Karasik, and A Sergeev, "Terahertz hot-electron micro-bolometer based on low-mobility 2-deg in GaN heterostructures," IEEE Sens. J. **13**(1), 80–88 (2013).
[23]M. C. Lemme, T. J. Echtermeyer, M. Baus, and H. Kurz, "A graphene field-effect device," IEEE Electron Device Lett. **28**(4), 282–284 (2007).